

RESEARCH

Open Access



# Compositionally and functionally distinct sinus microbiota in chronic rhinosinusitis patients have immunological and clinically divergent consequences

Emily K. Cope<sup>1,3</sup>, Andrew N. Goldberg<sup>1</sup>, Steven D. Pletcher<sup>1</sup> and Susan V. Lynch<sup>2\*</sup>

## Abstract

**Background:** Chronic rhinosinusitis (CRS) is a heterogeneous disease characterized by persistent sinonasal inflammation and sinus microbiome dysbiosis. The basis of this heterogeneity is poorly understood. We sought to address the hypothesis that a limited number of compositionally distinct pathogenic bacterial microbiota exist in CRS patients and invoke discrete immune responses and clinical phenotypes in CRS patients.

**Results:** Sinus brushings from patients with CRS ( $n = 59$ ) and healthy individuals ( $n = 10$ ) collected during endoscopic sinus surgery were analyzed using 16S rRNA gene sequencing, predicted metagenomics, and RNA profiling of the mucosal immune response. We show that CRS patients cluster into distinct sub-groups (DSI-III), each defined by specific pattern of bacterial co-colonization (permutational multivariate analysis of variance (PERMANOVA);  $p = 0.001$ ,  $r^2 = 0.318$ ). Each sub-group was typically dominated by a pathogenic family: *Streptococcaceae* (DSI), *Pseudomonadaceae* (DSII), *Corynebacteriaceae* [DSIII(a)], or *Staphylococcaceae* [DSIII(b)]. Each pathogenic microbiota was predicted to be functionally distinct (PERMANOVA;  $p = 0.005$ ,  $r^2 = 0.217$ ) and encode uniquely enriched gene pathways including ansamycin biosynthesis (DSI), tryptophan metabolism (DSII), two-component response [DSIII(b)], and the PPAR- $\gamma$  signaling pathway [DSIII(a)]. Each is also associated with significantly distinct host immune responses; DSI, II, and III(b) invoked a variety of pro-inflammatory,  $T_H1$  responses, while DSIII(a), which exhibited significantly increased incidence of nasal polyps (Fisher's exact;  $p = 0.034$ , relative risk = 2.16), primarily induced IL-5 expression (Kruskal Wallis;  $q = 0.045$ ).

**Conclusions:** A large proportion of CRS patient heterogeneity may be explained by the composition of their sinus bacterial microbiota and related host immune response—features which may inform strategies for tailored therapy in this patient population.

**Keywords:** Microbiome, Sinus, Airway, Chronic rhinosinusitis, Cystic fibrosis, Colonization patterns, Predicted metagenome, Dirichlet state, Microbiota state, Microbiota

## Background

The field of human microbiome research has profoundly altered our view of the diversity of human-associated microbes and encoded functions, and demonstrated that the microbiome co-varies with host health status [1–3]. In healthy subjects, a diverse bacterial microbiota

colonizes the upper respiratory mucosal surface [4, 5], and the lower airways possess a low burden and diversity of bacteria [6]. In contrast, patients with chronic inflammatory airway disease exhibit opposing trends in bacterial diversity and burden and compositionally distinct mucosal microbiota, enriched for known or suspected pathogenic species, and related to features of pulmonary disease [1, 5, 7, 8]. Chronic rhinosinusitis (CRS), characterized by persistent inflammation of the sinonasal mucosa lasting at least 12 weeks, is a common and

\* Correspondence: Susan.Lynch@ucsf.edu

<sup>2</sup>Division of Gastroenterology, Department of Medicine, University of California, San Francisco, CA 94143, USA

Full list of author information is available at the end of the article

refractory respiratory disease [9, 10], not least because of the immunologic and clinical heterogeneity exhibited by these patients. Until recently, little was known of the microbiome of the sinus mucosa in either healthy subjects or diseased patients. However, several recent culture-independent studies have now demonstrated that loss of sinus microbiota diversity is a common feature of patients with CRS [5, 11, 12] and, independently, that greater pre-operative sinus microbiota diversity is associated with improved post operative outcomes [13]. Respiratory pathogens such as *Pseudomonas aeruginosa* or *Staphylococcus aureus* are commonly isolated from CRS patients [14], while pathobionts, such as *Corynebacterium tuberculosis-terricum*, also found to be enriched in CRS patients, have demonstrable capacity to induce sinus mucosal infection in murine models [5]. However, these pathogens do not exist in isolation, but in mixed-species mucosal microbiota, the composition and activities of which, we hypothesize, explain the substantial clinical and immunological heterogeneity observed in CRS patients.

Previous efforts to explain CRS patient heterogeneity have been based on clinical [15, 16], immunologic [17–20], or pathologic [21] endotypes, though these studies have been relatively small and focused on specific immune cell populations or clinical features. More recently airway studies have examined whether subject stratification based on microbiota composition offers an improved approach for understanding immunological or clinical phenotypic variation across populations. A large study ( $n = 234$ ) of the infant nasopharyngeal microbiota identified six compositionally distinct microbiota, each dominated by a common respiratory bacterial genus and associated with significantly different relative risk for acute upper respiratory infection or development of asthma at 5 years [4]. Similarly, three compositionally and functionally distinct pathogenic lung microbiota have been described in HIV-infected pneumonia patients ( $n = 182$ ), each co-associate with a specific host immune response profile and differ in mortality risk [22]. Moreover, predicted metabolic products characteristic of each of these three distinct pathogenic lower airway communities were found to be enriched in paired serum samples, indicating that the microbiome of the overtly colonized airway may actively contribute both to local and systemic immune and metabolic dysfunction. The capacity for meaningful stratification based on microbiota composition is perhaps most compelling in a recent study of 1-month-old infants ( $n = 130$ ), who were divisible into three distinct gut microbiota states, one of which conferred a three-fold increased risk of atopy at the age of 2 years and asthma at the age of 4 years. The associated products of the high-risk microbiota induced CD4 + IL4+ cell population expansion and CD4 + CD25 + FoxP3+ suppression ex vivo [23]. Hence, several lines of investigation

suggest that patient immunological status and clinical outcomes differ significantly based on the specific microbiota structure present. Given these observations, we hypothesized CRS patient heterogeneity may be explained by the presence of distinct pathogenic sinus microbiota that invoke discrete host immune responses and relate to clinical phenotypes. To address this hypothesis, we examined the sinus mucosal microbiome and parallel host immune responses of a cohort of CRS and healthy subjects and related these findings to clinical outcomes of nasal polyposis. We demonstrate the presence of distinct pathogenic sinus microbiota in CRS patients each predicted to encode unique functional attributes, which co-associate with specific innate and adaptive immune responses, and significantly different relative risk of nasal polyposis.

## Methods

### Study design

The UCSF Institutional Review Board (approval number 11-07750) approved this study. All participants were informed of the objectives of this study and signed a written consent form prior to their participation. Adult patients ( $n = 76$ ) undergoing endoscopic sinus surgery (ESS) for CRS were enrolled at the University of California San Francisco. Samples from two patients did not yield PCR product, and five patients were removed from the analysis due to low sequence depth. Therefore, 69 subjects (10 healthy, 59 CRS patients) were included in downstream analysis (Table 1).

### Patient enrollment and sample collection

Disease was clinically diagnosed according to the 2007 Rhinosinusitis Task Force guidelines [24], and severity was radiographically quantified using the Lund-Mackay Computed Tomography (CT) scoring system. All CRS patients had symptoms for more than 12 consecutive weeks and CT evidence of inflammation within a month of sampling for this study. Patient demographics are described in Table 1. Recent clinical history, sinonasal outcomes test (SNOT-20), and CT sinus review were collected and used to confirm CRS diagnosis. Recent antibiotic use and intraoperative antibiotic administrations were recorded at the time of sample collection. Co-morbidities, including physician-diagnosed asthma or cystic fibrosis (CF), were recorded. Sinus brushings were obtained for 11 control patients undergoing surgery for non-CRS etiologies including oral surgery, trans-sphenoidal pituitary surgery, or endoscopic cerebral spinal fluid leak repair. Endoscopically guided protected brushes (ConMed #149, NY) were used to collect mucosal samples of the diseased sinus by brushing each surface gently while rotating the brush five times. Each sample was immediately placed in 1 ml of RNA later, transferred to 4 °C for 24–48 h

**Table 1** Demographics of CRS patients and healthy subjects included in this study

Sample ID	Age	Gender	Disease	Pre-operative antibiotics $\leq 3$ months	Lund-Mackay score	Polyp	Status
33	47	F	CRS+CF	Multiple ( $\geq 3$ )	22	N	Included
36	27	F	CRS+CF	Multiple ( $\geq 3$ )	18	Y	Included
39	28	M	CRS+CF	Multiple ( $\geq 3$ )	13	N	Included
61	20	M	CRS+CF	Azithromycin	15	Y	Included
64	71	M	CRS+CF	Dicloxacillin	16	Y	Included
83	24	M	CRS+CF	Multiple	19	Y	Included
90	20	F	CRS+CF	Ceftriaxone	19	Y	Included
91	47	M	CRS+CF	Zithromax/dapsone	17	Y	Included
108	30	M	CRS+CF	Multiple ( $\geq 3$ )	16	Y	Included
1	41	M	CRS	Augmentin	5	N	Included
7	39	F	CRS	Augmentin	12	N	Included
8	55	F	CRS+Asthma	Augmentin	23	Y	Included
15	55	M	CRS+Asthma	Clarithromycin	15	N	Included
16	51	M	CRS	Augmentin	22	N	Included
17	61	F	CRS+Asthma	Multiple ( $\geq 3$ )	12	N	Included
22	58	M	CRS+Asthma	Bactrim	12	Y	Included
32	19	M	CRS	Augmentin	22	Y	Included
34	51	M	CRS+Asthma	Levofloxacin	5	N	Included
40	72	F	CRS	Tobramycin	9	N	Included
43	46	M	CRS	Augmentin	12	N	Included
44	62	M	CRS	Levofloxacin	20	Y	Included
54	71	M	CRS+Asthma	dicloxacillin	13	Y	<10,000 sequences/sample
55	68	F	CRS+Asthma	Clotrimazole	21	Y	Included
56	67	F	CRS	Augmentin/Bactrim	14	Y	Included
58	85	M	CRS	Ampicillin/sulbactam	ND <sup>a</sup>	ND	No PCR product
59	42	F	CRS+Asthma	Clindamycin	4	Y	Included
60	35	M	CRS	Multiple ( $\geq 3$ )	16	N	Included
63	77	F	CRS	Levofloxacin	6	N	Included
80	58	M	CRS	Augmentin	8	N	Included
81	65	F	CRS+Asthma	Augmentin	10	N	Included
82	28	M	CRS	Augmentin	9	Y	Included
85	24	F	CRS+Asthma	Augmentin	4	N	Included
86	88	F	CRS	None	19	Y	Included
88	73	M	CRS	None	21	Y	Included
89	52	M	CRS	Clarithromycin	ND	ND	No PCR product
92	59	M	CRS	Multiple ( $\geq 3$ )	13	N	Included
93	48	M	CRS	Azithromycin/augmentin	11	Y	Included
94	72	F	CRS+Asthma	Augmentin	8	N	Included
96	54	M	CRS	Cephalexin	11	Y	Included
97	52	M	CRS	Cetirizine	22	Y	Included
98	39	M	CRS+Asthma	Multiple ( $\geq 3$ )	16	Y	Included
99	57	M	CRS	Levofloxacin	16	Y	Included
100	62	F	CRS	Bactrim	4	N	Included
101	27	M	CRS+Asthma	Azithromycin	ND	Y	Included

**Table 1** Demographics of CRS patients and healthy subjects included in this study (Continued)

103	36	M	CRS	Augmentin	10	Y	Included
104	23	M	CRS	None	12	N	Included
105	18	M	CRS	None	21	N	Included
107	37	F	CRS	Cephalexin	7	Y	Included
109	71	M	CRS+Asthma	Augmentin	11	Y	Included
110	18	F	CRS	Multiple ( $\geq 3$ )	16	N	Included
111	59	M	CRS	Augmentin	10	N	Included
112	48	F	CRS	Augmentin	9	N	Included
114	37	F	CRS	Clindamycin	1	N	Included
115	26	F	CRS	Augmentin	3	N	Included
117	33	M	CRS	Ciprofloxacin	19	N	Included
120	50	F	CRS+Asthma	Multiple ( $\geq 3$ )	15	Y	Included
121	33	F	CRS	Augmentin	9	Y	Included
122	45	F	CRS+Asthma	Augmentin	21	Y	Included
123	74	M	CRS+Asthma	Augmentin	16	Y	Included
124	30	M	CRS+Asthma	Augmentin	6	N	<10,000 sequences/sample
126	43	F	CRS+Asthma	Augmentin	11	Y	<10,000 sequences/sample
128	69	M	CRS+Asthma	Bactrim	21	Y	Included
130	59	M	CRS+Asthma	Augmentin	17	Y	Included
132	48	M	CRS	Rifampin	13	N	<10,000 sequences/sample
143	61	M	CRS	Augmentin	ND	N	Included
30	38	M	Healthy	Topical bacitracin	ND	N	<10,000 sequences/sample
31	59	M	Healthy	Amoxicillin/azithromycin	ND	N	Included
131	59	F	Healthy <sup>b</sup>	None	1	N	Included
CRS14	41	M	Healthy <sup>b</sup>	None	ND	N	Included
CRS15	39	M	Healthy	None	ND	N	Included
CRS16	37	F	Healthy	None	ND	N	Included
CRS17	46	F	Healthy	None	ND	N	Included
CRS18	46	M	Healthy	None	ND	N	Included
CRS19	31	F	Healthy	None	ND	N	Included
CRS20	18	F	Healthy	None	ND	N	Included
ctrl4	22	M	Healthy	None	ND	N	Included

<sup>a</sup>ND not determined<sup>b</sup>Allergic rhinitis

to permit the nucleic acid preservative to permeate cells prior to storage at  $-80^{\circ}\text{C}$  [25].

#### DNA extraction

Nucleic acids were extracted as previously described using the AllPrep kit (Qiagen, CA), to purify DNA and RNA in parallel [5, 25]. Briefly, brushes were placed in Lysis Matrix B tubes in 600  $\mu\text{l}$  Buffer RLT Plus with  $\beta$ -mercaptoethanol and bead beaten for 30 s at  $5.5\text{ m sec}^{-1}$  for nucleic acid extraction per manufacturer's protocol. DNA and RNA were quantified using a NanoDrop 2000 (ThermoFisher, CA). DNA concentrations were normalized to  $50\text{ ng }\mu\text{l}^{-1}$  per

sample for 16S rRNA gene sequence library preparation, described below.

#### 16S rRNA gene library preparation

Barcoded primers 515 F/806R were used to amplify the V4 region of the 16S rRNA gene as previously described [26, 27]. Since double bands were present, one human mitochondrial band and a microbial 16S band, amplicons of the correct size (384 bp) were gel-extracted with a Qiagen Gel Extraction kit per manufacturer protocol. Purified PCR product was analyzed on Bioanalyzer (Aligent, CA, USA), quantified using the Qubit HS dsDNA kit (Invitrogen, CA, USA), and pooled at 25 ng per sample.

The pooled library was quantified using the KAPA QPCR Illumina Library Quantification kit (KAPA Biosystems, MA, USA), diluted to 2 nM, denatured, and 5 pM was loaded onto the Illumina MiSeq cartridge (V2) in combination with a 15% (*v/v*) of denatured 12.5 pM PhiX spike-in. In addition to negative control extraction blanks, a mock community composed of equal genomic concentration (2 ng each per reaction) of *Escherichia coli* ATCC25922, *P. aeruginosa* ATCC27853, *C. tuberculoearicum* ATCC35692, *Lactobacillus sakei* ATCC15521, and *L. rhamnosus* ATCC53103 was also used to monitor runs.

### 16S rRNA gene sequence processing

Sequence analysis of 16S rRNA data was performed using Quantative Insights Into Microbial Ecology (QIIME) version 1.8.0 [28] and in the R environment. See Supplemental Methods for details.

### Sequence and statistical analyses

Since our rarefaction curves approached an asymptote (indicating adequate community coverage) at a sequence depth 10,055 sequences, and all but 5 samples were sequenced at least to this depth, the operational taxonomic unit (OTU) table was multiple rarefied to 10,055 high-quality, chimera-checked sequences per sample for subsequent analyses using a custom script (<https://github.com/alifar76/MicroNorm>). All subsequent analyses were performed on this rarefied table. UniFrac, Canberra, and Bray-Curtis dissimilarity matrices were generated in QIIME 1.8.0, and Principal Coordinates Analysis (PCoA) plots were used to visualize ordinations using emperor [29]. Permutational multivariate analysis of variance (PERMANOVA) using the *adonis* function in the R Vegan package was used to determine significance in dissimilarity matrices across samples by metadata categories (e.g., disease, Dirichlet state, antibiotic use, age, and disease severity [30, 31]). Faith's phylogenetic diversity, number of unique OTUs (richness), and Pielou's evenness were calculated and a permutational *t* test (999 Monte Carlo permutations) was used to determine changes in alpha diversity. When multiple comparisons were performed, we corrected for false discovery using the Benjamini-Hochberg method and reported the corrected *p* values as *q* values, a  $q \leq 0.05$  was considered significant [32]. Changes in taxon relative abundance were determined per OTU using a zero-inflated negative binomial (<https://github.com/alifar76/NegBinSig-Test>) distribution on a regression model. Kruskal-Wallis was used to determine if statistically significant differences in OTU or Kyoto Encyclopedia of Genes and Genomes (KEGG) pathway abundances existed between more than two groups, such as healthy patients, CRS, and CRS+CF patients. To identify clusters, the Dirichlet-multinomial

mixture probabilistic community modeling was performed using the *DirichletMultinomial* package [33] in R with family-level taxonomy using absolute abundances of each family. The Laplace approximation was used to calculate model fit and to determine the number of components (clusters). Distinct sample clusters that represented the best model fit were termed Dirichlet states (DS). To determine whether DSIII could be separated into two phylogenetically distinct groups, hierarchical cluster analysis was performed on a weighted UniFrac distance matrix using an edited version of *pvclust* in R (code attached in Additional file 1, Additional file 2, Additional file 3, Additional file 4, Additional file 5). Kruskal-Wallis was used to determine whether host genes were significantly up- or down-regulated in disease. Statistical analysis was performed using R.

### Predicted metagenomics

Metagenome prediction from the closed-reference OTUs (greengenes 13\_5) of the multiple rarefied OTU table was performed using the Phylogenetic Investigation of Communities by Reconstruction of Unobserved States (PICRUSt v. 1.0.0 [34]). QIIME 1.8.0 was used to analyze the predicted metagenomes. Differential abundances of pathways were tested using a Kruskal-Wallis test when comparing more than two groups or a three-model approach (negative binomial, zero-inflated negative binomial, or poisson distributions) applied on a regression to test pairwise comparisons. Model fit was determined using Akaike information criterion (AIC) values, and the associated statistic was reported (<https://github.com/alifar76/NegBinSig-Test>). Nearest Sequenced Taxon Index (NTSI) scores were calculated using the `-a` flag in `metagenome_predictions.py`. These represent the average branch length separating OTUs in a sample from a reference bacterial genome. A heatmap was constructed for KEGG categories that were enriched or depleted in each disease state using `heatmap.3` in R. For visualization, read counts were normalized [ $\log_2(x + 1)$ ] and scaled by row. See Additional file 6: Supplemental Methods for more detail.

### Quantitative PCR for bacterial burden and human gene expression

Quantitative PCR (qPCR) was used to quantify bacterial burden as a ratio to human beta-actin. See Supplemental Methods for primers and PCR conditions. A custom qPCR array was developed (SA Biosciences, Hilden, Germany) and used to quantify host gene expression using RNA extracted in parallel from patient sinus brushes. See Additional file 6: Supplemental Methods



for gene targets and reverse transcriptase (RT) PCR conditions.

## Results

### Sinus mucosal microbiome perturbations characterize

#### CRS and are related to disease status

Our cohort consisted of 76 subjects. Sixty-five were CRS patients and 11 were healthy subjects. CRS patients included those with concomitant lower airway disease i.e. cystic fibrosis (CRS+CF) or asthma (CRS+A; Table 1). Sinus brushing samples from 2 subjects yielded no 16S rRNA amplicons (both from CRS patients), and a further 5 samples were removed due to low sequence depth (<10,000 sequences/sample;  $n = 4$  CRS and  $n = 1$  healthy). Thus, 10 healthy individuals and 59 CRS patients were included in the analyses presented.

CRS patients exhibited significantly higher Lund McKay scores compared to healthy subjects ( $p < 0.05$ ), however amongst CRS patients, disease severity did not differ based on the presence or absence of concomitant lower airway disease (Tukey's post hoc comparison;  $p > 0.05$ , Additional file 6: Figure S1A). Mucosal bacterial burden (based on total 16S rRNA copy number) was not significantly different across healthy and CRS patients (ANOVA;  $p = 0.781$ ; Fig. 1a), consistent with previous reports [5, 12]. Also consistent with previous findings [5, 12] was the observation that compared with healthy

subjects, CRS patients exhibited significantly lower microbiota richness, evenness, and diversity. Of note, diminished alpha diversity in CRS patients was more pronounced in those with concomitant lower airway disease (permutational  $t$  test; all  $p < 0.01$ ; Fig. 1b–d). Multivariate analysis (PERMANOVA) of sinus bacterial beta diversity on a weighted UniFrac distance matrix was used to determine whether factors such as age, antimicrobial administration, polyposis, revision surgery (a complete list is provided in Table 2) explained the observed variation in community composition across all subjects (CRS and healthy), or exclusively within the CRS patients. Of these, only disease status (healthy, CRS, CRS+CF, CRS+A) was significantly related to beta diversity, but only explained a small portion of microbiota compositional variance and the effect size was small (PERMANOVA;  $p = 0.001$ , 8.9% of variation explained, Fig. 1e; Table 2).

### Discrete pathogenic sinus microbiota exists in CRS patients

We postulated that the microbiota dysbiosis exhibited by CRS patients does not represent a single state, but rather a gradient of dysbioses punctuated by a limited number of distinct pathogenic microbiota compositional states. We addressed this hypothesis through the application of an unbiased probabilistic model, Dirichlet-multinomial mixtures (DMM) [33] which identifies clusters of samples

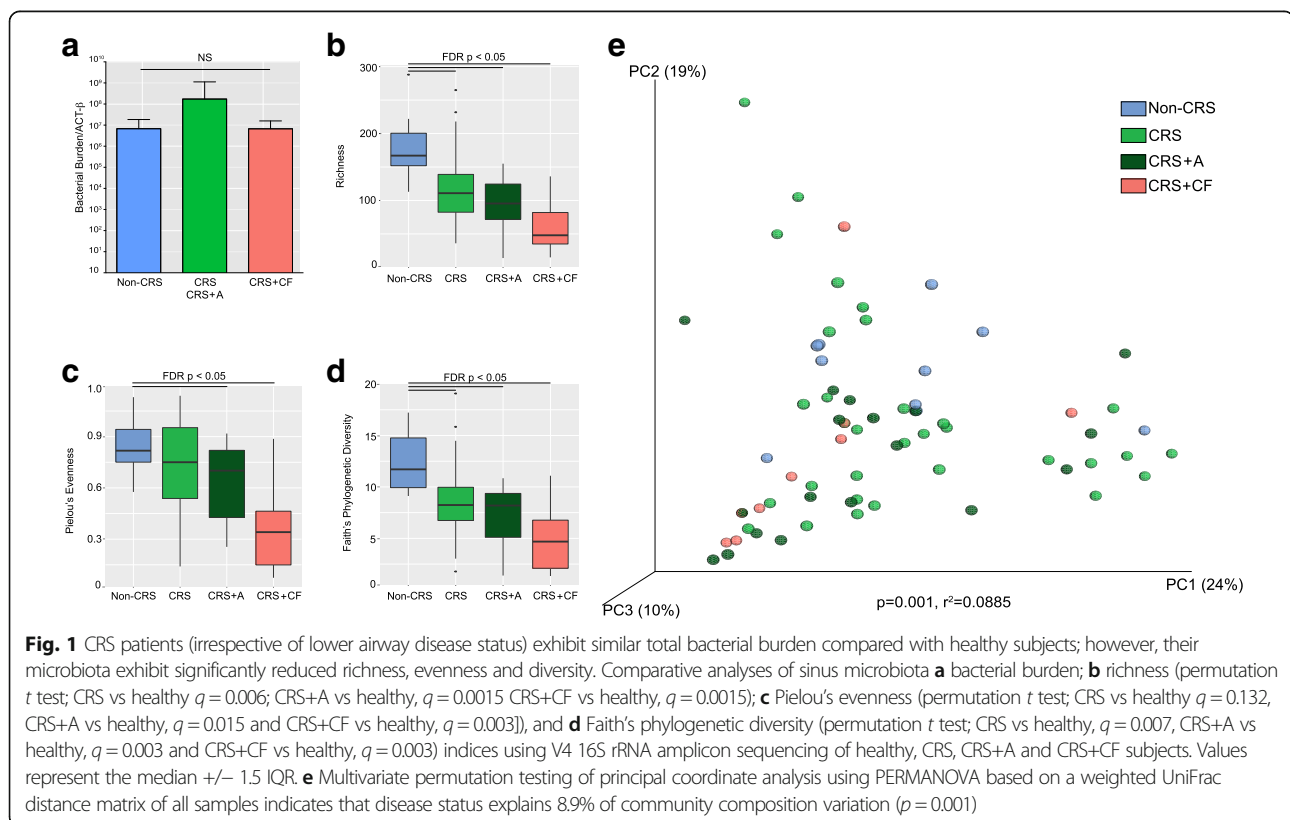


**Table 2** Multivariate analysis (PERMANOVA) of sinus bacterial beta diversity on a weighted UniFrac distance matrix

PERMANOVA (patient cohort)	$r^2$	$p$ value
<b>Dirichlet state (disease<sup>a</sup>)</b>	<b>0.326</b>	<b>0.001</b>
<b>Dirichlet state (all<sup>b</sup>)</b>	<b>0.318</b>	<b>0.001</b>
<b>Disease (all)</b>	<b>0.088</b>	<b>0.014</b>
Antibiotic use <3 months (disease)	0.036	0.052
Polyp presence/absence (disease)	0.025	0.152
Anatomic location (all)	0.039	0.185
Age bin 10 year (all)	0.118	0.196
Antibiotic class <3 months (all)	0.260	0.24
Age bin 5 year (all)	0.153	0.367
Antibiotic class <3 months (disease)	0.286	0.399
Anatomic location (disease)	0.0348	0.403
Age bin 10 year (disease)	0.119	0.473
Age bin 5 year (disease)	0.168	0.521
LMS Bin (low/medium/high) (disease)	0.046	0.554
Revision surgery (Y/N) (disease)	0.042	0.668
Age (disease)	0.674	0.799
Lund-Mackay score (LMS) (disease)	0.327	0.906
Age (all)	0.561	0.944

<sup>a</sup>CRS, CRS+CF, CRS+A<sup>b</sup>Healthy, CRS, CRS+A, CRS+CFThose in boldface are significant (the  $r^2$  value indicates the degree of community variance explained by the specific factor)

based on bacterial community composition. Based on a Laplace approximation, three distinct sample clusters, termed Dirichlet states (DSI-III) represented the best model fit (Additional file 6: Figure S3A); DSI comprised 26 subjects ( $n = 9/10$  healthy,  $n = 17$  CRS), DSII comprised 14 CRS patients, and DSIII comprised 28 CRS patients and one healthy subject. Upon chart review, it was noted that this particular healthy subject had allergic rhinitis. DS clusters were confirmed as compositionally distinct by PERMANOVA (weighted UniFrac PERMANOVA;  $p = 0.001$ , 31.8% variation; Fig. 2a), a finding that was robust irrespective of the distance matrix used to analyze the 16S rRNA data (Table 3, Additional file 6: Figure S2A). Both weighted and unweighted UniFrac distance matrices significantly explained DS-defined sample clustering, indicating that both bacterial phylogeny and rarer taxa in these communities discriminated DS groups. To further confirm this, sequence reads associated with the dominant family in each sample were removed and the data reanalyzed. DS classification remained significantly related to community composition (weighted UniFrac PERMANOVA;  $p = 0.001$ , 18.2% variation; Additional file 6: figure S2B) indicating that patterns of co-associated lower abundance taxa are discrete and relatively conserved within each of the three DS microbiota.

The proportion of healthy subjects and CRS patients with or without pulmonary co-morbidities varied significantly across DSI-III (Chi-squared;  $p = 0.0007$ ; Fig. 2b), with DSI possessing the least and DSII the greatest proportion of CRS patients with concomitant lower airway disease (CRS+CF and CRS+A). This implicates a co-association between specific pathogenic sinus community states and lower airway disease and also provides the first evidence that specific pathogenic sinus microbiota are common to both CF and asthmatic patients. While recent antibiotic use trended towards significance, it only explained a very minor portion of community compositional variance (PERMANOVA;  $p = 0.052$ ,  $r^2 = 0.036$ ; Table 2) and did not differ across DSI-III (Chi-squared;  $p = 0.149$ ). This is likely because these microbiota exist in antimicrobial resistant biofilms on the sinus mucosal surface [35]. Disease severity, as measured by Lund-Mackay radiographic scores also did not differ across DSI-III (ANOVA  $p = 0.825$ ), suggesting that distinct pathogenic microbiota may drive equally severe disease symptoms, albeit via distinct mechanisms (it should be noted that these patients were undergoing functional endoscopic sinus surgery at the time of sample collection).

DSIII was the largest group and was comprised of patients whose sinus mucosal microbiota represented a compositional continuum dominated by either *Staphylococcaceae* (*Firmicutes*) or *Corynebacteriaceae* (*Actinobacteria*). Since these taxa are phylogenetically distinct, are known competitors in the upper airways [36, 37], and elicit unique immune responses [38], we identified *Corynebacteriaceae*- or *Staphylococcaceae*-dominated patients within this group as distinct DSIII sub-groups, identified as DSIII(a) ( $n = 9$ ) or III(b) ( $n = 19$ ; Fig. 2b), respectively. This sub-grouping strategy was statistically supported by hierarchical clustering analysis on a weighted UniFrac distance matrix (au,  $p < 0.05$ ; Additional file 6: Figure S3B), and we confirmed the existence of a reciprocal relationship between *Corynebacteriaceae* [DSIII(a)] and *Staphylococcaceae* [DSIII(b)] relative abundance across DSIII samples (Additional file 6: Figure S3C).

Each pathogenic microbiota state (DSI-III) was characteristically dominated by a distinct bacterial family that co-associated with a relatively unique suite of lower abundance taxa (Fig. 2c). To identify taxonomic differentials characteristic of each CRS microbiota state, each was compared to healthy subjects using zero-inflated negative binomial (ZINB) regression (Fig. 2d–g, Additional file 3). The identity and magnitude of depleted taxa was relatively consistent irrespective of the CRS microbiota state examined and included *Streptococcus*, *Rothia*, *Haemophilus*, and *Lactobacillales* members (ZINB;  $p < 0.05$ ,  $q < 0.10$ ; Fig. 2d–g). The magnitude and types of taxa enriched in CRS patients differed by

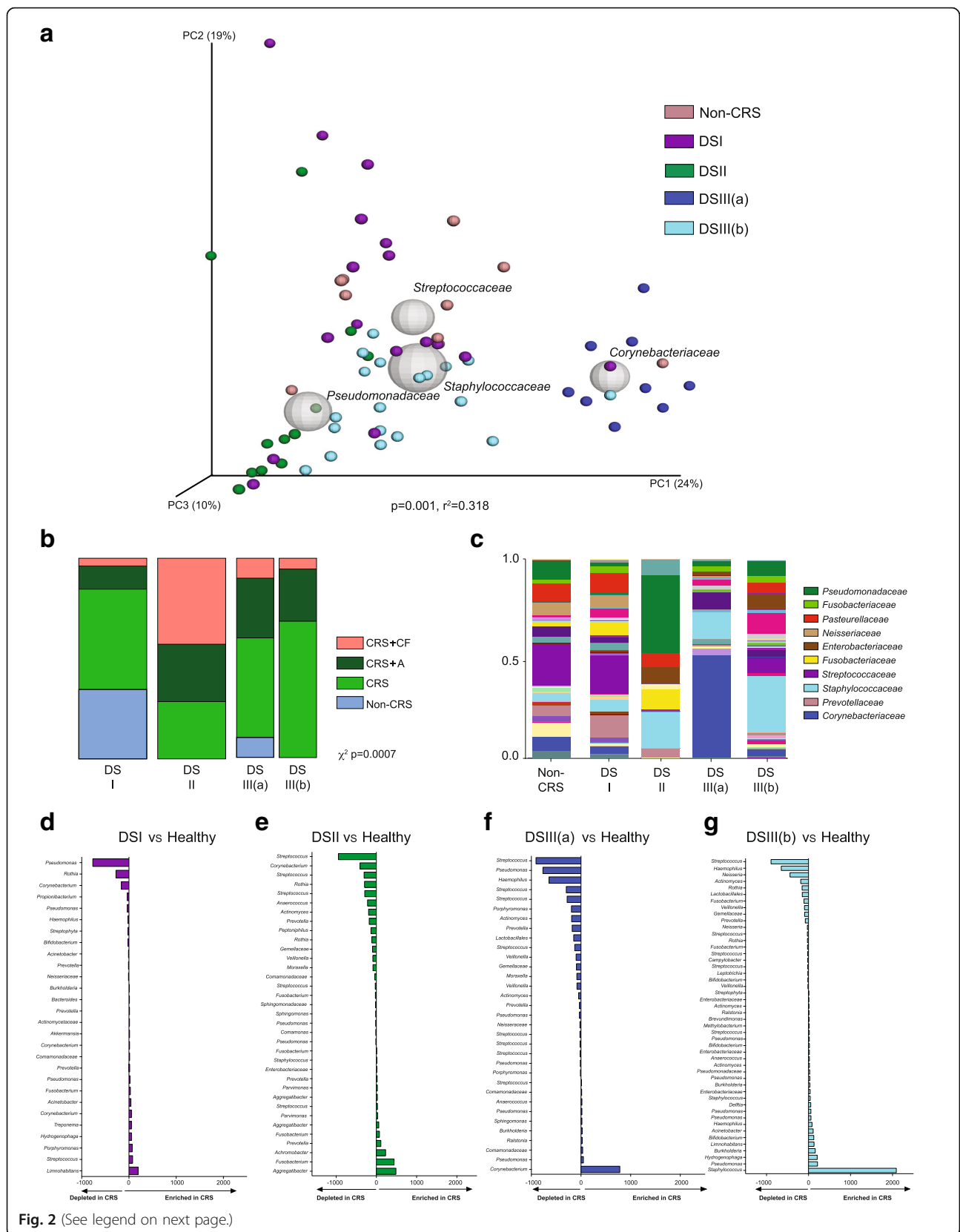


Fig. 2 (See legend on next page.)



(See figure on previous page.)

**Fig. 2** Dirichlet-multinomial mixtures modeling identifies microbial states that explain a large portion of variation in microbiota composition. **a** Multivariate permutation (PERMANOVA) testing of DS designation (I-III(b)) explains 31.8% of variation in sinus mucosal microbiota composition ( $p = 0.001$ ). The most abundant family-level taxa are indicated. Size of sphere is proportional to the average relative abundance of each dominant taxon. **b** Distribution of co-morbidities (CF or physician-diagnosed asthma) significantly differ across microbiota states. DSI was represented by CRS patients and 9/10 of the healthy controls. DSII was enriched for CRS+CF and CRS+A patients, whereas DSIII was composed primarily of CRS patients without concomitant lower airway disease, and one healthy control subject (Chi-squared;  $p = 0.0007$ ). **c** Stacked bar chart indicating the distribution of taxa in the sinuses grouped by DS. **d-g** Three-model testing of differential taxon abundance indicates that each DS is associated with enrichment for specific taxa and co-colonizers and depletion of microbiota associated with healthy individuals (ZINB;  $p < 0.05$ ,  $q < 0.10$ )

community state (Fig 2c) and were most pronounced in DSIII(a) and III(b), which exhibited relatively large *Corynebacterium* or *Staphylococcus* enrichments, respectively. DSI, though most compositionally similar to healthy controls, exhibited relative enrichment of *Streptococcus* as well as *Porphyromonas*, *Tannerella*, *Treponema*, *Bacteroides*, *Dialister*, and *Akkermansia* (ZINB;  $p < 0.05$ ,  $q < 0.05$ ). DSII, dominated by *Pseudomonadaceae*, was also relatively enriched for *Fusobacterium*, *Aggregatibacter*, *Achromobacter*, and *Prevotella* (ZINB;  $p < 0.05$ ,  $q < 0.05$ ), known airway pathobionts characteristically enriched in CF and asthmatic lungs [1, 7, 39, 40]. Presumably, this reflects the increased number of such patients in this subgroup and indicates that archetypal lower airway microbiome dysbioses in CF and asthmatic patients may also be reflected in the upper airway bacterial community composition of these patients. While DSIII(a) and III(b) shared substantial taxonomic overlap, explaining their statistical grouping into a single DMM cluster, DSIII(a) was uniquely enriched for *Sphingomonas* (ZINB;  $p < 0.0001$ ,  $q < 0.0001$ ; Fig. 2f) and DSIII(b) uniquely co-enriched for eight taxa absent in III(a) [*Actinobacteria*, *Bifidobacterium*, *Haemophilus*, *Enterobacteriaceae*, *Pseudomonadaceae*, *Sphingomonadaceae* (unclassified genus), *Selenomonas*, and *Streptophyta*] (ZINB;  $p < 0.05$ ,  $q < 0.05$ ; Fig. 2g).

Because the majority of healthy individuals were classified into DSI, we also compared DSII, III(a) and III(b) individually to DSI. General concordance was observed between taxa enriched in DSII or III when compared to either DSI or healthy subjects (ZINB;  $p < 0.05$ ,  $q < 0.05$ ; Additional file 6: Tables S1-S3). The primary discriminating genera for each DS remained consistent; differences were only observed in a select few low abundance taxa, validating the observation that the DSI microbiota was compositionally similar to that of healthy subjects. When compared to DSI, DSII remained enriched for

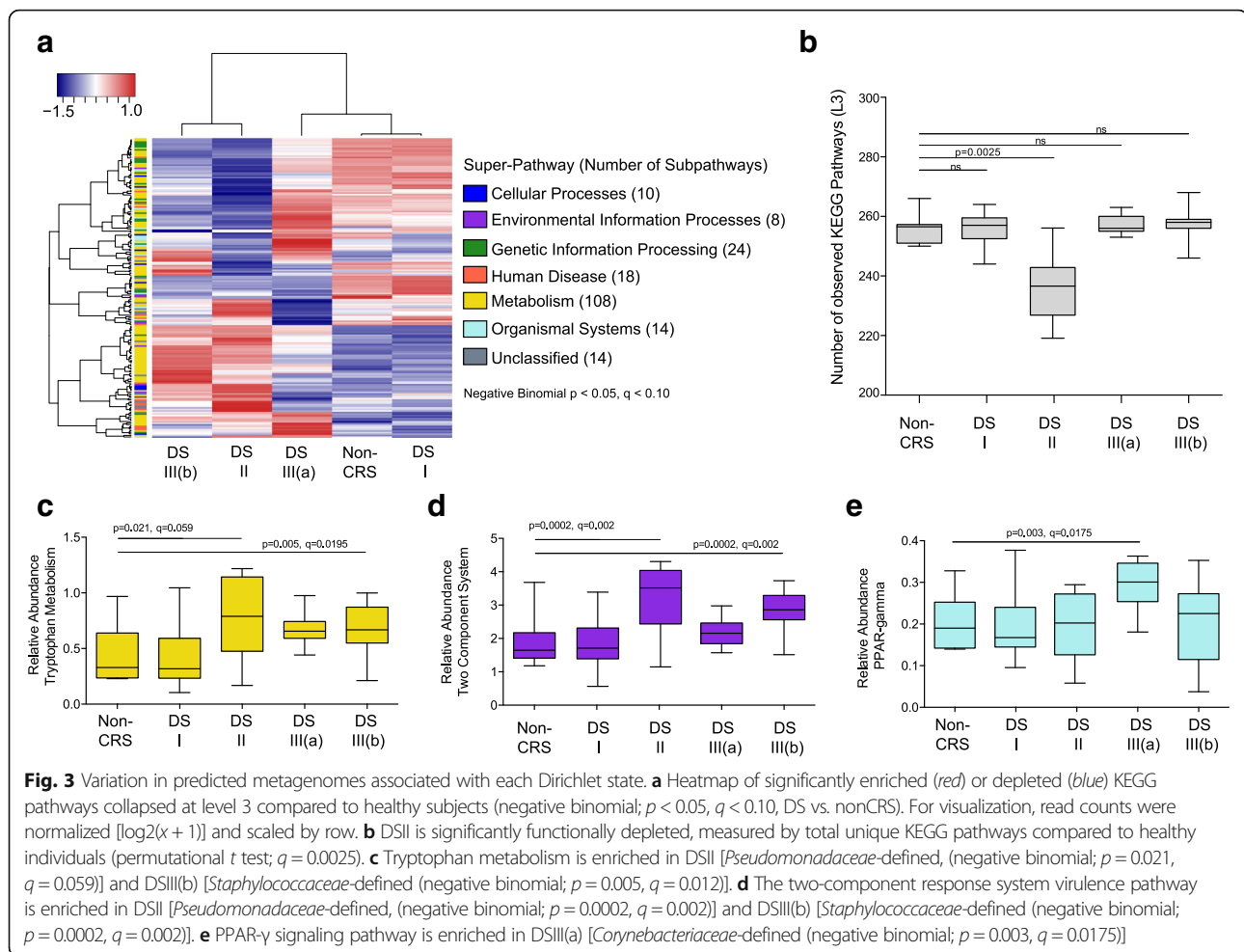
*Aggregatibacter*, *Achromobacter*, *Fusobacterium*, and *Prevotella* but was also relatively enriched for *Pseudomonas* (ZINB;  $p = 0.004$ ,  $q = 0.026$ ). DSIII(a) and III(b) remained highly enriched for *Corynebacterium* or *Staphylococcus* although *Cloacibacterium* were uniquely co-enriched with *Corynebacterium* and *Serratia* were uniquely co-enriched with *Staphylococcus* when these groups were compared with DSI.

#### Predicted functional capacity discriminates sinus bacterial Dirichlet states

Bacterial metagenomes were predicted *in silico* for each patient using PICRUSt, an algorithm which uses biomarker gene sequence data i.e., 16S rRNA to infer evolutionarily conserved functional gene capacity using representative sequenced and predicted ancestral genomes. Associated Nearest Sequenced Taxon Index (NTSI) scores which indicate the degree of relatedness between OTUs and sequenced genomes used for PICRUSt predictions are detailed in Additional file 7. Each microbiota state was predicted to encode a distinct metagenome (Bray-Curtis PERMANOVA;  $p = 0.001$ , 23.2% variation explained; Additional file 6: Figure S4) and a total of 196 KEGG pathways differentiated pathogenic microbiota states compared control patients (three-model test;  $p < 0.05$ ,  $q < 0.10$ ; Fig. 3a). Only 21 KEGG pathways discriminated patients with distinct lower airway comorbidities (asthma+/-, CF; Kruskal-Wallis;  $p < 0.05$ ,  $q < 0.10$ ; Additional file 6: Table S4), indicating substantial overlap in sinus microbiota function in the upper airways of CRS patients with distinct lower airway diseases. Compared to healthy microbiota, the DSII group was the least functionally diverse (permutational  $t$  test;  $q < 0.05$ ; Fig. 3b) and depleted of 67 KEGG pathways for lipid, carbohydrate, terpenoid, and xenobiotic metabolism. DSII and III(b) were both significantly enriched in bacterial virulence pathways, including two-component response systems, and for fatty acid and tryptophan metabolism pathways associated with inflammation (negative binomial;  $p < 0.05$ ,  $q < 0.05$ ; Fig. 3c-d, Additional file 6: Table S5), when compared to healthy controls. DSI patients were depleted of polyketide and folate biosynthesis and enriched for a pathway responsible for ansamycin biosynthesis, a

**Table 3** Weighted and unweighted UniFrac distance matrix

PERMANOVA (Dirichlet states)	$r^2$	$p$ value
Weighted UniFrac	0.326	0.001
Unweighted UniFrac	0.182	0.001
Bray-Curtis	0.195	0.001
Canberra	0.099	0.001



microbial secondary metabolite with a broad range antimicrobial activity (poison;  $p < 0.0001$ ,  $q < 0.0001$ ; Additional file 6: Table S5A) [41]. *Corynebacterium*-dominated DSIII(a) was characterized by both peroxisome proliferator-activated receptor- $\gamma$  (PPAR- $\gamma$ ) (negative binomial;  $p = 0.003$ ,  $q = 0.018$ ; Fig. 3e, Additional file 6: Table S5C) and the retinoic acid-inducible gene-1 (RIG-I) signaling pathways (negative binomial;  $p = 0.015$ ,  $q = 0.062$ ; Additional file 6: Table S5C), both of which have been shown to be increased in eosinophilic polyp tissue in CRS patients [42, 43].

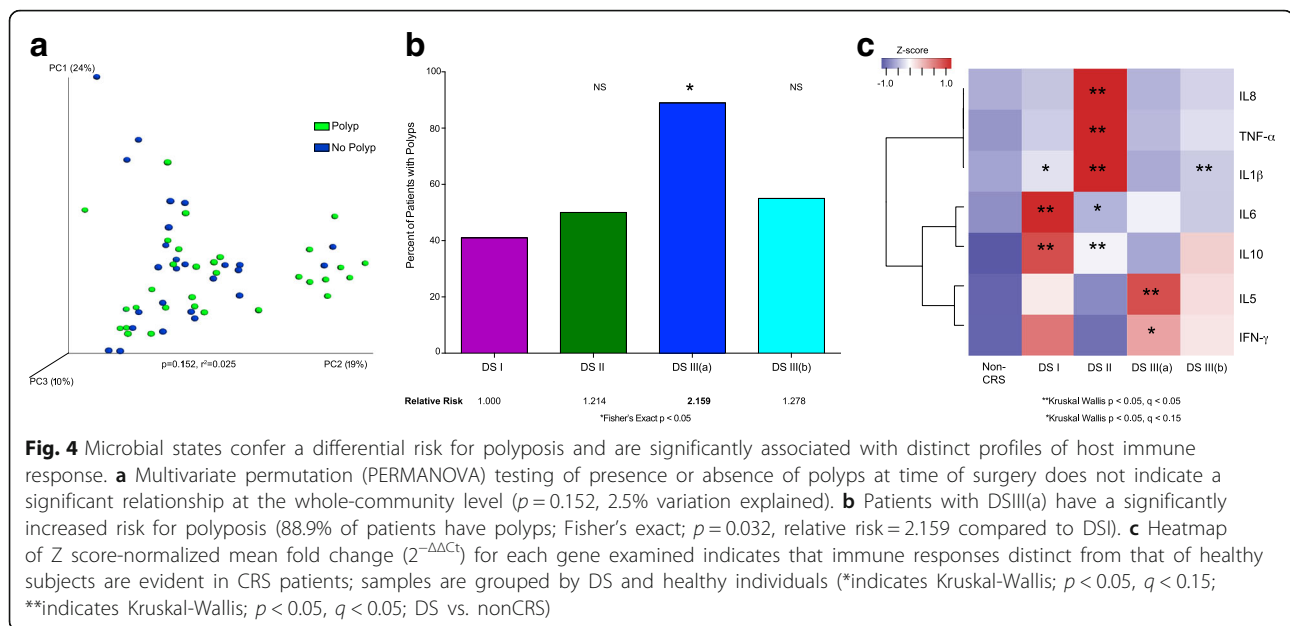
#### Sinus microbial communities correlate with clinical outcomes

Bacterial community composition within the cohort did not correlate with polyposis (weighted UniFrac; PERMANOVA;  $p = 0.152$ , 2.5% variation; Fig 4a). However, based on the microbiota and predicted metagenome data, specifically, the enrichment of RIG-I and PPAR- $\gamma$  signaling pathways (previously associated with polyposis) in the *Corynebacterium*-dominated DSIII(a) patients, we predicted that these patients would exhibit significantly increased incidence of polyposis. We therefore performed

an assessment of polyp relative risk across microbiologically discrete CRS patient sub-groups compared to DSII patients, who possessed compositionally similar microbiota to those of healthy subjects and the lowest incidence of polyposis (41%; 7 of 17 patients). As expected, the DSIII(a) sub-group exhibited a significantly higher relative risk of polyposis compared to all of the other microbiologically defined patient sub-groups, with 89% (8 of 9 patients) of patients in this group exhibiting polyposis (Fisher's exact; relative risk = 2.159,  $p = 0.039$ ; Fig 4b).

#### Bacterial co-colonization patterns correlate with patterns of host gene expression

To determine, as we hypothesized, whether distinct DS-induced discrete host immune responses, we used qPCR to measure expression of innate and adaptive genes previously associated with CRS (Th1, Th2, Th17 and Treg cytokines, mucin, and epithelial barrier genes) using RNA extracted in parallel with DNA used to profile microbial communities from sinus brushings of all subjects. Fold change in gene expression (compared to healthy



subjects) was used to generate a multivariate immune response profile for each subject.

Each CRS DS group exhibited a significantly distinct host immune response, the specifics of which varied across CRS patient sub-groups (Fig. 4c; full array in Additional file 6: Figure S5). DSI, II, and III(b) patients exhibited significantly increased *IL-1β*, implicating macrophage and inflammasome involvement in these patients. In addition to *IL-1β*, patients in DSII also exhibited increased *IL-6*, *TNF-α*, *IL-8*, and *IL-10* expression (Kruskal-Wallis;  $p < 0.05$ ,  $q < 0.05$ ), suggestive of an epithelial/endothelial and/or macrophage-driven mucosal inflammatory response. DSI patients, whose microbiota composition differed subtly in taxonomic content from healthy individuals, were immunologically distinct and exhibited significantly increased *IL-1β*, *IL-6*, and *IL-10* compared to healthy individuals (Kruskal-Wallis;  $p < 0.05$ ,  $q < 0.05$ ). Thus, subtle taxonomic differences may influence the activity of this microbiota, or, alternatively, non-bacterial microbiota members may contribute to immune-stimulation in this subset of patients. DSIII(a) patients who are at higher relative risk for polyposis and whose sinus mucosal microbiome was enriched for *Corynebacterium* and predicted to encode PPAR- $\gamma$  and RIG-I signaling pathways were the only group to exhibit a significant increase in *IL-5* expression (Kruskal-Wallis;  $p < 0.05$ ,  $q < 0.05$ ; Fig 4d). *IL-5* is a potent activator of eosinophils, the dominant immune cell type in polyp tissue in Western populations of CRS patients [44]. Furthermore, these patients also had increased levels of *IFN-γ* (Kruskal-Wallis;  $p = 0.017$ ,  $q = 0.107$ ), which has been associated with non-eosinophilic polyposis [45].

Collectively, these findings indicate that distinct dysbiotic pathogenic bacterial microbiota states exist in CRS patient sub-groups that differ in relative risk for polyposis and induce discrete immune responses related to their clinical phenotypes.

## Discussion

Clinical diagnosis of CRS is somewhat subjective and often does not correlate well with patient outcomes [19]. Improved stratification of patients offers the opportunity to better tailor therapeutic regimens and advance towards the ultimate goal of personalized therapy. A previous study of the CRS-associated microbiota demonstrated evidence for mucosal microbiota collapse in patients with severe disease and enrichment of *C. tuberculo* [5]. That study also noted that though the number of CRS patients was very small, they parsed into two distinct groups based on sinus microbiota composition. In the current study, we validate previous findings and extend them, demonstrating that the CRS bacterial microbiota can exist in at least four distinct taxonomic states (one of which is dominated by *Corynebacteriaceae*). We suspect that these represent a gradient of pathogenic microbial co-colonizations that are related to patient treatment history and/or disease progression. Previous CRS microbiota studies have described high inter-patient taxonomic variability and dominance of common respiratory pathogens *Corynebacterium*, *Staphylococcus*, *Pseudomonas*, and anaerobes such as *Fusobacterium* and members of *Prevotellaceae* [11–13, 46, 47]. These genera also feature prominently in our study, but we expand upon these findings to demonstrate that these respiratory pathogens co-associate with distinct and reproducible microbial partners and explain a large proportion of the

observed inter-personal microbiota variation in CRS patients. These microbiologically distinct states are predicted to encode different metagenomes, are associated with a characteristic innate and adaptive host immune response, and differ significantly in the incidence of nasal polyposis, an important clinical phenotype of CRS.

Approximately one fifth of CRS patients had a mucosal microbiota characteristically enriched for *Corynebacteriaceae* and depleted of *Streptococcus*. Lemon and colleagues recently demonstrated that *Corynebacterium accolens*, a common skin commensal, metabolizes triacylglycerols in nasal secretions to oleic and linoleic acid, which inhibits *Streptococcus pneumoniae* growth [48]. Metagenome predictions indicated that the *Corynebacteriaceae* OTUs in dysbiotic CRS patient microbiota also encode the capacity for linoleic acid biosynthesis, suggesting that this mechanism of *Streptococcus* inhibition may play a role in deterministically shaping the pattern of co-colonizing species around this dominant respiratory pathogen in the chronically inflamed sinus microbiota. However, further in vitro and in vivo studies are required to determine whether this mechanism plays a role in defining CRS microbiota composition. Independent of this pathway, a recently described phylogenetic-related species, *Corynebacterium pyruviciproducens*, has been shown to stimulate dendritic cell maturation and proliferation and up-regulate Th2 responses in mice [49]. Additionally, the lipoarabinomannan-based lipoglycans of *Corynebacterium glutamicum* induce Th17 responses via TLR2 recognition on dendritic cells [50], indicating several discrete pathogenic pathways exist in this genus. In our study, *Corynebacteriaceae*-defined microbial communities were enriched in PPAR- $\gamma$  and RIG-I pathways. PPAR- $\gamma$ , a lipid-sensing receptor, controls gene expression and metabolism and has recently been shown to regulate eosinophil activation in polyp tissue of CRS patients [42]. It has also been associated with asthma [51] and airway remodeling following allergic inflammation in mice [52]. RIG-I, an intracellular sensor of viral DNA, is elevated in nasal polyp tissue [43] and is induced by *IFN- $\gamma$*  [53]. Consistent with these observations, patients possessing a *Corynebacteriaceae*-dominated community state were uniquely associated with increased *IL-5* and *IFN- $\gamma$*  gene expression and were at a higher risk for developing polyposis. Mounting evidence suggests that members of this family, particularly in the context of a taxonomically and functionally depleted sinus microbiota, represent a group of underappreciated pathobionts, whose activities induce T<sub>H</sub>2-skewed immune responses.

Of the remaining DMM-identified microbial states, patients classified into DSII (*Pseudomonadaceae*-dominated) were the least functionally diverse, the most immunologically active, and housed the greatest proportion of CF and asthma patients, who also commonly exhibit

lower airway microbiota dominated by this family. Predicted functional enrichments in DSII included pathways involved in tryptophan metabolism and lipopolysaccharide biosynthesis, both of which induce host inflammatory responses [54]. For example, recent studies have demonstrated that HIV-infected patients with the greatest degree of peripheral immune activation are enriched for *Pseudomonas* species in their gastrointestinal microbiota and that isolates of *Pseudomonas* from these patients exhibit the capacity to catabolize tryptophan to pro-inflammatory kynurenine in vitro [55, 56]. Interestingly, other co-colonizing members of the DSII community are known producers of tryptophan e.g., *Achromobacter* [57], implicating metabolic cross-feeding between the dominant respiratory pathogen and its co-colonizers as a deterministic mechanism that plausibly underlies their frequent co-association in *Pseudomonas*-dominated sinus microbiota. Additionally, tryptophan metabolites increase biofilm formation [58, 59] and virulence gene expression [60, 61], indicating that enhanced capacity for the production and metabolism of this crucial amino acid by co-associated members of this community state may be critical to enhanced antimicrobial resistance and pathogenicity. Immunologically, patients in DSII, which had the highest prevalence of CRS+CF patients, exhibited increases in genes associated with neutrophil and macrophage activation, including *TNF- $\alpha$*  and *IL-8*, which is consistent with CF airway immune responses associated with strains of *P. aeruginosa* specifically adapted to the lung environment [62, 63]. *IL-1 $\beta$*  gene expression was increased in DSI, II, and III(b), which may indicate a role for inflammasome activation in CRS patients with T<sub>H</sub>1-skewed disease. Inflammasomes are multi-meric protein complexes that assemble in cells to control the production of *IL-1 $\beta$*  and *IL-18* following activation by pathogen-associated molecular patterns (PAMPs), such as peptidoglycan [64].

The goal of this study was to better understand CRS patient heterogeneity by leveraging high-resolution microbiota profiles to stratify patients into discrete subgroups and to determine whether such a stratification strategy explained immunological and clinical outcomes in these patients as has been demonstrated in other chronic diseases [4, 22, 23, 65]. We demonstrate the existence of distinct microbiota states and show that they are robust and encode unique functional attributes that correlate with mucosal immune responses and clinical outcomes. We recognize that this cross-sectional study cannot address whether these microbiota states are stable or transient; however, it is plausible that they represent a gradient of pathogenic bacterial community successional states associated with disease progression. It will be interesting to determine whether medical management of CRS, such as antimicrobial treatment or



surgery, alters a patient's microbiota state and associated inflammatory response towards that of a different conformation and whether the states we have identified are in fact related to disease progression or duration. Antibiotics can rapidly and pervasively shift the composition of the microbiota in the human gut [66, 67] and can influence sinus microbial composition, at least in the short term [68]. Future studies will examine the effects of medical and surgical management of CRS on the stability of the disease microbiota. Although concomitant lower airway co-morbidities (asthma or CF) explained a small portion of beta diversity variation, we demonstrate that some asthmatics and cystic fibrosis patients share the same sinus microbiota state. This observation suggests that subsets of patients with clinically distinct respiratory diseases share the same pathogenic microbiota and host immune response. The concept that discrete respiratory diseases have overlapping pathophysiology has been recently explored in asthma and chronic obstructive pulmonary disease (COPD) [69, 70]. Our data suggests this phenomenon may extend to CF and be explained, at least in part, by overlapping microbiota colonization states. Furthermore, enrichment of *Proteobacteria* in the lower airways patients with established asthma or CF is well documented [7, 71, 72]; our findings demonstrate that lower airway bacterial biomarkers of these respiratory diseases exist in the upper respiratory tract, which may represent a source of pathogenic microbes for lower airway colonization. Future studies will incorporate more thoroughly characterized asthmatics, since asthma immune subtypes are well described and may plausibly be explained by the microbiota states observed in our study [73].

In this initial study, we did not profile viral or fungal components of these microbiota states, which also likely play a role in driving the observed bacterial heterogeneity or host immune response. We also recognize the limitations of using a predictive algorithm to infer metagenome content, particularly since PICRUSt has been most thoroughly studied in the GI tract, (though PICRUSt predictions on nasal samples from the Human Microbiome Project have been shown to be robust when compared to shotgun metagenome sequencing [33]). Future studies will use shotgun metagenomics and transcriptomics approaches to confirm PICRUSt-predicted metagenomes as well as to identify viral and fungal taxa in these patients. We anticipate that metagenomics, in parallel with metabolomics and transcriptomics will substantially improve our capacity to meaningfully stratify patients based on their microbiome.

We observed a non-significant trend towards an association between antibiotic usage and microbiota composition in our study. It is possible that this study was not sufficiently powered to find an association between

antibiotic use and microbial composition and that the compositional differences between CRS and healthy subjects may, at least in part, be antibiotic-mediated. We are continuing to recruit patients and will examine this possibility in larger cohorts of cases and controls. Finally, though the precise cellular source of the cytokines induced by the pathogenic bacterial community states cannot be gleaned from our gene expression studies of human sinus mucosa, we identified significantly up-regulated genes associated with each state that warrant further investigation. Despite these limitations, the microbial and immunological features described herein provide an explanation for CRS patient heterogeneity and provide a foundation for improved understanding of how distinct pathogenic sinus microbiota may collectively and distinctly drive mucosal disease processes in CRS patients.

## Conclusions

Heterogeneity among CRS patients is poorly understood and represents a significant barrier to disease treatment and to the development of more effective therapies. This study validates and extends previous findings that show collapse of mucosal-associated microbiota in CRS patients [5, 12, 47]. Here, we demonstrate that CRS microbiota can exist in at least four compositional states that are predicted to have distinct functional attributes, correlate with distinct host immune responses, and associate with differential risk for nasal polyps, an important clinical disease phenotype. The presence of *Corynebacteriaceae*-dominant microbial communities in CRS patients were associated with increased *IL-5* gene expression and increased risk for nasal polyps while the remaining three microbial community states were immunologically diverse and were not associated with polyp risk. These findings support prior studies that characterize the immunological heterogeneity of CRS patients using similar clustering approaches [20], but by examining microbial signatures, our studies may provide an explanation for these diverse immune profiles that exist within this patient population. The microbial and immunological features described here may inform strategies for tailored therapy in this patient population.

## Additional files

**Additional file 1:** Edited pvclust R code for use with a precomputed distance matrix. (R 13 kb)

**Additional file 2:** Workflow of commands for pvclust. (R 1 kb)

**Additional file 3:** Source file (1) for pvclust. (R 7 kb)

**Additional file 4:** Source file (2) for pvclust. (R 13 kb)

**Additional file 5:** Read me file for pvclust. (TXT 908 bytes)

**Additional file 6:** Supplemental Information. **Figure S1A.** Lund-MacKay scores associated with disease state. No differences were observed



between CRS, CRS+A or CRS+CF patients; B. CRS-CF patients are significantly younger than CRS+A patients (ANOVA, Tukey's  $p = 0.041$ ); however, no differences in age were observed for pairwise comparisons between the other groups ( $p > 0.05$ , Tukey's post hoc test). **Figure S2A.** PCoA of an unweighted UniFrac distance matrix colored by DS-IIIb and healthy (PERMANOVA  $p = 0.001$ , 18.2% variation explained); B. PCoA of weighted UniFrac distance matrix after dominant sequence reads associated with the dominant family in each sample were removed demonstrating that DS still significantly explains variation in community composition despite removal of the dominant taxon from each sample (PERMANOVA  $p = 0.001$ , 17.6% variation explained).

**Figure S3A.** Laplace model fit demonstrates three distinct Dirichlet multinomial mixtures groups. B. Hierarchical cluster analysis using a weighted-UniFrac distance matrix showing that microbiomes enriched in *Corynebacteriaceae* forms a distinct cluster (au  $p = 100$ ). Heatmap shows relative abundance of the bacterial general that comprise >90% of the total sequence reads. C. Reciprocal relationship between *Corynebacteriaceae* and *Staphylococcaceae*. **Figure S4.** PICRUSt-predicted functional variation across microbial Dirichlet states shows significant functional differences A. PCoA of Canberra distance matrix; PERMANOVA  $p = 0.001$ , 21.7% of variation explained) B. PCoA of Bray-Curtis distance matrix; PERMANOVA  $p = 0.001$ , 22.0% of variation explained). **Figure S5.** Expression levels of all host immune genes measured by qPCR (\*indicates Kruskal-Wallis  $p < 0.05$ ,  $q < 0.15$ ; \*\*indicates Kruskal-Wallis  $p < 0.05$ ,  $q < 0.05$ ; DS vs. nonCRS).

**Table S1–S5.** (ZIP 1671 kb)

**Additional file 7:** Nearest Taxon Sequence Index (NTSI) scores for PICRUSt predictions. (XLSX 41 kb)

## Abbreviations

AIC: Akaike information criterion; CF: Cystic fibrosis; CRS: Chronic rhinosinusitis; CT: Computed tomography; DMM: Dirichlet-multinomial mixtures model; DS: Dirichlet state; KEGG: Kyoto Encyclopedia of Genes and Genomes; NTSI: Nearest taxon sequence identity; OTU: Operational taxonomic unit; PCoA: Principal Coordinates Analysis; PERMANOVA: Permutational multivariate analysis of variance

## Acknowledgements

We thank the patients who provided samples for this study and to the members of the Lynch Lab for their thoughtful discussions regarding this study. We'd like to thank K. Fujimura for her helpful comments on the manuscript, J. Mar for help modifying *pvclust*, and A. Faruqi for his three-model and multiple rarefaction scripts.

## Funding

EKC and SVL are supported by a Cystic Fibrosis Foundation Award. ANG and SDP are supported by private donation.

## Availability of data and materials

Sequence data is deposited in the European Nucleotide Archive (<http://www.ebi.ac.uk/ena>) under study accession number PRJEB20232

## Authors' contributions

EKC, SVL, ANG, and SDP all developed the study concept and design. EKC carried out DNA/RNA isolation, 16S rRNA gene library preparation, sequence analysis, interpreted the microbiome/immune data, and wrote the manuscript. SVL interpreted the microbiome and immune data, guided statistical analysis, as well as wrote and critically reviewed the manuscript. ANG and SDP recruited patients and collected specimens, collected clinical metadata, interpreted the microbiome data, and were major contributors in writing the manuscript and reviewing it critically. All authors read and approved the final manuscript.

## Authors' information

Not applicable.

## Competing interests

The authors declare that they have no competing interests.

## Consent for publication

Not applicable.

## Ethics approval and consent to participate

The UCSF Institutional Review Board (approval number 11-07750) approved this study. All participants were informed of the objectives of this study and signed a written consent form prior to their participation.

## Publisher's Note

Springer Nature remains neutral with regard to jurisdictional claims in published maps and institutional affiliations.

## Author details

<sup>1</sup>Department of Otolaryngology, University of California, San Francisco, CA 94143, USA. <sup>2</sup>Division of Gastroenterology, Department of Medicine, University of California, San Francisco, CA 94143, USA. <sup>3</sup>Present Address: Pathogen and Microbiome Institute, Northern Arizona University, Flagstaff, AZ 86011, USA.

Received: 20 January 2017 Accepted: 18 April 2017

Published online: 12 May 2017

## References

- Huang YJ, Nelson CE, Brodie EL, Desantis TZ, Baek MS, Liu J, Woyke T, Allgaier M, Bristow J, Wiener-Kronish JP, et al. Airway microbiota and bronchial hyperresponsiveness in patients with suboptimally controlled asthma. *J Allergy Clin Immunol*. 2011;127(2):372–81. e371–373.
- Morgan XC, Tickle TL, Sokol H, Gevers D, Devaney KL, Ward DV, Reyes JA, Shah SA, LeLeiko N, Snapper SB, et al. Dysfunction of the intestinal microbiome in inflammatory bowel disease and treatment. *Genome Biol*. 2012;13(9):R79.
- Yatsunen T, Rey FE, Manary MJ, Trehan I, Dominguez-Bello MG, Contreras M, Magris M, Hidalgo G, Baldassano RN, Anokhin AP, et al. Human gut microbiome viewed across age and geography. *Nature*. 2012;486(7402):222–7.
- Teo SM, Mok D, Pham K, Kusel M, Serralha M, Troy N, Holt BJ, Hales BJ, Walker ML, Hollans E, et al. The infant nasopharyngeal microbiome impacts severity of lower respiratory infection and risk of asthma development. *Cell Host Microbe*. 2015;17(5):704–15.
- Abreu NA, Nagalingam NA, Song Y, Roediger FC, Pletcher SD, Goldberg AN, Lynch SV. Sinus microbiome diversity depletion and *Corynebacterium tuberculoostearicum* enrichment mediates rhinosinusitis. *Sci Transl Med*. 2012;4(151):151ra124.
- Charlson ES, Bittinger K, Haas AR, Fitzgerald AS, Frank I, Yadav A, Bushman FD, Collman RG. Topographical continuity of bacterial populations in the healthy human respiratory tract. *Am J Respir Crit Care Med*. 2011;184(8):957–63.
- Huang YJ, Nariya S, Harris JM, Lynch SV, Choy DF, Arron JR, Boushey H. The airway microbiome in patients with severe asthma: associations with disease features and severity. *J Allergy Clin Immunol*. 2015;136(4):874–84.
- Simpson JL, Daly J, Baines KJ, Yang IA, Upham JW, Reynolds PN, Hodge S, James AL, Hugenoltz P, Willner D, et al. Airway dysbiosis: *Haemophilus influenzae* and *Tropheryma* in poorly controlled asthma. *Eur Respir J*. 2016; 47(3):792–800.
- Fokkens WJ, Lund VJ, Mullol J, Bachert C, Alobid I, Baroody F, Cohen N, Cervin A, Douglas R, Gevaert P et al. European position paper on rhinosinusitis and nasal polyps 2012. *Rhinol Suppl*. 2012;23(3):1–298.
- Caulley L, Thavorn K, Rudmik L, Cameron C, Kilty SJ. Direct costs of adult chronic rhinosinusitis by using 4 methods of estimation: results of the US Medical Expenditure and Survey. *J Allergy Clin Immunol*. 2015;136(6):1517–22.
- Kim RJ, Biswas K, Hoggard M, Taylor MW, Douglas RG. Paired analysis of the microbiota of surface mucus and whole-tissue specimens in patients with chronic rhinosinusitis. *Int Forum Allergy Rhinol*. 2015;5(10):877–83.
- Biswas K, Hoggard M, Jain R, Taylor MW, Douglas RG. The nasal microbiota in health and disease: variation within and between subjects. *Front Microbiol*. 2015;9:134.
- Ramakrishnan VR, Hauser LJ, Feazel LM, Ir D, Robertson CE, Frank DN. Sinus microbiota varies among chronic rhinosinusitis phenotypes and predicts surgical outcome. *J Allergy Clin Immunol*. 2015;136(2):334–42. e331.
- Bendouah Z, Barbeau J, Hamad WA, Desrosiers M. Biofilm formation by *Staphylococcus aureus* and *Pseudomonas aeruginosa* is associated with an unfavorable evolution after surgery for chronic sinusitis and nasal polyposis. *Otolaryngol Head Neck Surg*. 2006;134(6):991–6.
- Divekar R, Patel N, Jin J, Hagan J, Rank M, Lal D, Kita H, O'Brien E. Symptom-based clustering in chronic rhinosinusitis relates to history of aspirin

- sensitivity and postsurgical outcomes. *J Allergy Clin Immunol Pract.* 2015; 3(6):934–40. e933.
16. Lal D, Rounds AB, Rank MA, Divekar R. Clinical and 22-item sino-nasal outcome test symptom patterns in primary headache disorder patients presenting to otolaryngologists with "sinus" headaches, pain or pressure. *Int Forum Allergy Rhinol.* 2015;5(5):408–16.
  17. Derycke L, Eyerich S, Van Crombruggen K, Perez-Novo C, Holtappels G, Deruyck N, Gevaert P, Bachert C. Mixed T helper cell signatures in chronic rhinosinusitis with and without polyps. *PLoS One.* 2014;9(6):e97581.
  18. Yang Y, Zhang N, Crombruggen KV, Lan F, Hu G, Hong S, Bachert C. Differential expression and release of activin a and follistatin in chronic rhinosinusitis with and without nasal polyps. *PLoS One.* 2015;10(6):e0128564.
  19. Akdis CA, Bachert C, Cingi C, Dykewicz MS, Hellings PW, Naclerio RM, Schleimer RP, Ledford D. Endotypes and phenotypes of chronic rhinosinusitis: a PRACTALL document of the European Academy of Allergy and Clinical Immunology and the American Academy of Allergy, Asthma & Immunology. *J Allergy Clin Immunol.* 2016;131(6):1479–90.
  20. Tomassen P, Vandeplass G, Van Zele T, Cardell LO, Arebro J, Olze H, Forster-Ruhmann U, Kowalski ML, Olszewska-Ziaber A, Holtappels G, et al. Inflammatory endotypes of chronic rhinosinusitis based on cluster analysis of biomarkers. *J Allergy Clin Immunol.* 2016;137(5):1449–56. e1444.
  21. Tan NC, Cooksley CM, Roscioli E, Drilling AJ, Douglas R, Wormald PJ, Vreugde S. Small-colony variants and phenotype switching of intracellular *Staphylococcus aureus* in chronic rhinosinusitis. *Allergy.* 2014;69(10):1364–71.
  22. Shenoy MK, Iwai S, Lin DL, Worodria W, Ayakaka I, Byanyima P, Kaswabuli S, Fong S, Stone S, Chang E et al. Immune response and mortality risk relate to distinct lung microbiomes in HIV-pneumonia patients. *Am J Respir Crit Care Med.* 2017;195(1):104–14.
  23. Fujimura KE, Sitarik AR, Havstad S, Lin DL, Levan S, Fadrosch D, Panzer AR, LaMere B, Rackaityte E, Lukacs NW, et al. Neonatal gut microbiota associates with childhood multisensitized atopy and T cell differentiation. *Nat Med.* 2016;22(10):1187–91.
  24. Rosenfeld RM. Clinical practice guideline on adult sinusitis. *Otolaryngol Head Neck Surg.* 2007;137(3):365–77.
  25. Roediger FC, Slusher NA, Allgaier S, Cox MJ, Pletcher SD, Goldberg AN, Lynch SV. Nucleic acid extraction efficiency and bacterial recovery from maxillary sinus mucosal samples obtained by brushing or biopsy. *Am J Rhinol Allergy.* 2010;24(4):263–5.
  26. Caporaso JG, Lauber CL, Walters WA, Berg-Lyons D, Huntley J, Fierer N, Owens SM, Betley J, Fraser L, Bauer M, et al. Ultra-high-throughput microbial community analysis on the Illumina HiSeq and MiSeq platforms. *ISME J.* 2012;6(8):1621–4.
  27. Caporaso JG, Lauber CL, Walters WA, Berg-Lyons D, Lozupone CA, Turnbaugh PJ, Fierer N, Knight R. Global patterns of 16S rRNA diversity at a depth of millions of sequences per sample. *Proc Natl Acad Sci U S A.* 2011; 108 Suppl 1:4516–22.
  28. Caporaso JG, Kuczynski J, Stombaugh J, Bittinger K, Bushman FD, Costello EK, Fierer N, Pena AG, Goodrich JK, Gordon JJ, et al. QIIME allows analysis of high-throughput community sequencing data. *Nat Methods.* 2010;7(5):335–6.
  29. Vazquez-Baeza Y, Pirrung M, Gonzalez A, Knight R. EMPPer: a tool for visualizing high-throughput microbial community data. *Gigascience.* 2013;2(1):16.
  30. Oksanen J, Blanchet F.G., Kindt R., Legendre P., Minchin, P.R., O'Hara, R.B., Simpson, G.L., Solymos, P., Stevens, H.H., Wagner, H. *Vegan: community ecology package.* R package version 20-10 2013.
  31. Anderson MJ. A new method for non-parametric multivariate analysis of variance. *Austral Ecol.* 2001;26:32–46.
  32. Storey JD. A direct approach to false discovery rates. *J R Stat Soc B.* 2002;64:479–98.
  33. Holmes I, Harris K, Quince C. Dirichlet multinomial mixtures: generative models for microbial metagenomics. *PLoS One.* 2012;7(2):e30126.
  34. Langille MG, Zaneveld J, Caporaso JG, McDonald D, Knights D, Reyes JA, Clemente JC, Burkhead DE, Vega Thurber RL, Knight R et al. Predictive functional profiling of microbial communities using 16S rRNA marker gene sequences. *Nat Biotechnol.* 2013;31(9):814–21.
  35. Foreman A, Psaltis AJ, Tan LW, Wormald PJ. Characterization of bacterial and fungal biofilms in chronic rhinosinusitis. *Am J Rhinol Allergy.* 2009; 23(6):556–61.
  36. Lina G, Boutite F, Tristan A, Bes M, Etienne J, Vandenesch F. Bacterial competition for human nasal cavity colonization: role of *Staphylococcus* agr alleles. *Appl Environ Microbiol.* 2003;69(1):18–23.
  37. Yan M, Pamp SJ, Fukuyama J, Hwang PH, Cho DY, Holmes S, Relman DA. Nasal microenvironments and interspecific interactions influence nasal microbiota complexity and *S. aureus* carriage. *Cell Host Microbe.* 2013;14(6):631–40.
  38. Kobayashi T, Glatz M, Horiuchi K, Kawasaki H, Akiyama H, Kaplan DH, Kong HH, Amagai M, Nagao K. Dysbiosis and *Staphylococcus aureus* colonization drives inflammation in atopic dermatitis. *Immunity.* 2015;42(4):756–66.
  39. Coburn B, Wang PW, Diaz Caballero J, Clark ST, Brahma V, Donaldson S, Zhang Y, Surendra A, Gong Y, Elizabeth Tullis D, et al. Lung microbiota across age and disease stage in cystic fibrosis. *Sci Rep.* 2015;5:10241.
  40. Madan JC, Koestler DC, Stanton BA, Davidson L, Moulton LA, Housman ML, Moore JH, Guill MF, Morrison HG, Sogin ML et al. Serial analysis of the gut and respiratory microbiome in cystic fibrosis in infancy: interaction between intestinal and respiratory tracts and impact of nutritional exposures. *MBio.* 2012;3(4).
  41. Evans SE, Goult BT, Fairall L, Jamieson AG, Ko Ferrigno P, Ford R, Schwabe JW, Wagner SD. The ansamycin antibiotic, rifamycin SV, inhibits BCL6 transcriptional repression and forms a complex with the BCL6-BTB/POZ domain. *PLoS One.* 2014;9(3):e90889.
  42. Asaka C, Honda K, Ito E, Fukui N, Chihara J, Ishikawa K. Peroxisome proliferator-activated receptor-gamma is expressed in eosinophils in nasal polyps. *Int Arch Allergy Immunol.* 2011;155 Suppl 1:57–63.
  43. Bogefors J, Kvarnhammar AM, Latif L, Petterson T, Uddman R, Cardell LO. Retinoic acid-inducible gene 1-like receptors in the upper respiratory tract. *Am J Rhinol Allergy.* 2011;25(6):e262–7.
  44. Bachert C, Wagenmann M, Hauser U, Rudack C. IL-5 synthesis is upregulated in human nasal polyp tissue. *J Allergy Clin Immunol.* 1997;99(6 Pt 1):837–42.
  45. Cho KS, Kim CS, Lee HS, Seo SK, Park HY, Roh HJ. Role of interferon-gamma-producing T cells in the pathogenesis of chronic rhinosinusitis with nasal polyps associated with staphylococcal superantigen. *J Otolaryngol Head Neck Surg.* 2010;39(5):600–5.
  46. Joss TV, Burke CM, Hudson BJ, Darling AE, Forer M, Alber DG, Charles IG, Stow NW. Bacterial communities vary between sinuses in chronic rhinosinusitis patients. *Front Microbiol.* 2015;6:1532.
  47. Hoggard M, Biswas K, Zoing M, Wagner Mackenzie B, Taylor MW, Douglas RG. Evidence of microbiota dysbiosis in chronic rhinosinusitis. *Int Forum Allergy Rhinol.* 2017;7(3):230–9.
  48. Bomar L, Brugger SD, Yost BH, Davies SS, Lemon KP. *Corynebacterium accolens* releases antipneumococcal free fatty acids from human nostril and skin surface triacylglycerols. *MBio.* 2016;7(1):e01725–15.
  49. Qingzhen H, Jia T, Shengjun W, Yang Z, Yanfang L, Pei S, Essien BS, Zhaoliang S, Sheng X, Qixiang S, et al. *Corynebacterium pyruviciproducens* promotes the production of ovalbumin specific antibody via stimulating dendritic cell differentiation and up-regulating Th2 biased immune response. *Vaccine.* 2012;30(6):1115–23.
  50. Mishra AK, Alves JE, Krumbach K, Nigou J, Castro AG, Geurtsen J, Eggeling L, Saraiva M, Besra GS. Differential arabinan capping of lipoarabinomannan modulates innate immune responses and impacts T helper cell differentiation. *J Biol Chem.* 2012;287(53):44173–83.
  51. Lee KS, Park SJ, Hwang PH, Yi HK, Song CH, Chai OH, Kim JS, Lee MK, Lee YC. PPAR-gamma modulates allergic inflammation through up-regulation of PTEN. *FASEB J.* 2005;19(8):1033–5.
  52. Honda K, Marquillies P, Capron M, Dombrowicz D. Peroxisome proliferator-activated receptor gamma is expressed in airways and inhibits features of airway remodeling in a mouse asthma model. *J Allergy Clin Immunol.* 2004;113(5):882–8.
  53. Imaizumi T, Tanaka H, Tajima A, Tsuruga K, Oki E, Sashinami H, Matsumiya T, Yoshida H, Inoue I, Ito E. Retinoic acid-inducible gene-1 (RIG-I) is induced by IFN-gamma in human mesangial cells in culture: possible involvement of RIG-I in the inflammation in lupus nephritis. *Lupus.* 2010;19(7):830–6.
  54. Harden JL, Lewis SM, Lish SR, Suarez-Farinas M, Gareau D, Lentini T, Johnson-Huang LM, Krueger JG, Lowes MA. The tryptophan metabolism enzyme L-tryptophanase is a novel inflammatory factor in psoriasis and other inflammatory diseases. *J Allergy Clin Immunol.* 2016;137(6):1830–40.
  55. Favre D, Mold J, Hunt PW, Kanwar B, Loke P, Seu L, Barbour JD, Lowe MM, Jayawardene A, Aweeka F, et al. Tryptophan catabolism by indoleamine 2,3-dioxygenase 1 alters the balance of TH17 to regulatory T cells in HIV disease. *Sci Transl Med.* 2010;2(32):32ra36.
  56. Vujkovic-Cvijin I, Dunham RM, Iwai S, Maher MC, Albright RG, Broadhurst MJ, Hernandez RD, Lederman MM, Huang Y, Somsouk M, et al. Dysbiosis of the gut microbiota is associated with HIV disease progression and tryptophan catabolism. *Sci Transl Med.* 2013;5(193):193ra191.
  57. Ujimar T, Kakimoto T, Chibata I. I-Tryptophan production by *Achromobacter liquidum*. *Appl Environ Microbiol.* 1983;46(1):1–5.

58. Sasaki-Imamura T, Yano A, Yoshida Y. Production of indole from L-tryptophan and effects of these compounds on biofilm formation by *Fusobacterium nucleatum* ATCC 25586. *Appl Environ Microbiol.* 2010;76(13):4260–8.
59. Lee J, Attila C, Cirillo SL, Cirillo JD, Wood TK. Indole and 7-hydroxyindole diminish *Pseudomonas aeruginosa* virulence. *Microb Biotechnol.* 2009;2(1):75–90.
60. Anyanful A, Dolan-Livengood JM, Lewis T, Sheth S, Dezalia MN, Sherman MA, Kalman LV, Benian GM, Kalman D. Paralysis and killing of *Caenorhabditis elegans* by enteropathogenic *Escherichia coli* requires the bacterial tryptophanase gene. *Mol Microbiol.* 2005;57(4):988–1007.
61. Hirakawa H, Kodama T, Takumi-Kobayashi A, Honda T, Yamaguchi A. Secreted indole serves as a signal for expression of type III secretion system translocators in enterohaemorrhagic *Escherichia coli* O157:H7. *Microbiology.* 2009;155(Pt 2):541–50.
62. Lubamba BA, Jones LC, O'Neal WK, Boucher RC, Ribeiro CM. X-box-binding protein 1 and innate immune responses of human cystic fibrosis alveolar macrophages. *Am J Respir Crit Care Med.* 2015;192(12):1449–61.
63. LaFayette SL, Houle D, Beaudoin T, Wojewodka G, Radzioch D, Hoffman LR, Burns JL, Dandekar AA, Smalley NE, Chandler JR et al. Cystic fibrosis-adapted quorum sensing mutants cause hyperinflammatory responses. *Sci Adv.* 2015;1(6).
64. Jones CL, Weiss DS. TLR2 signaling contributes to rapid inflammasome activation during *F. novicida* infection. *PLoS One.* 2011;6(6):e20609.
65. Makowska JS, Burney P, Jarvis D, Keil T, Tomassen P, Bislimovska J, Brozek G, Bachert C, Baelum J, Bindslev-Jensen C et al. Respiratory hypersensitivity reactions to NSAIDs in Europe: the global allergy and asthma network (GA2 LEN) survey. *Allergy.* 2016;71(11):1603–11.
66. Dethlefsen L, Relman DA. Incomplete recovery and individualized responses of the human distal gut microbiota to repeated antibiotic perturbation. *Proc Natl Acad Sci U S A.* 2011;108 Suppl 1:4554–61.
67. Theriot CM, Koenigsnecht MJ, Carlson Jr PE, Hatton GE, Nelson AM, Li B, Huffnagle GB JZL, Young VB. Antibiotic-induced shifts in the mouse gut microbiome and metabolome increase susceptibility to *Clostridium difficile* infection. *Nat Commun.* 2014;5:3114.
68. Liu CM, Soldanova K, Nordstrom L, Dwan MG, Moss OL, Contente-Cuomo TL, Keim P, Price LB, Lane AP. Medical therapy reduces microbiota diversity and evenness in surgically recalcitrant chronic rhinosinusitis. *Int Forum Allergy Rhinol.* 2013;3(10):775–81.
69. Postma DS, Rabe KF. The asthma-COPD overlap syndrome. *N Engl J Med.* 2015;373(13):1241–9.
70. Christenson SA, Steiling K, van den Berge M, Hijazi K, Hiemstra PS, Postma DS, Lenburg ME, Spira A, Woodruff PG. Asthma-COPD overlap. Clinical relevance of genomic signatures of type 2 inflammation in chronic obstructive pulmonary disease. *Am J Respir Crit Care Med.* 2015;191(7):758–66.
71. Marri PR, Stern DA, Wright AL, Billheimer D, Martinez FD. Asthma-associated differences in microbial composition of induced sputum. *J Allergy Clin Immunol.* 2013;131(2):346–52. e341-343.
72. Bacci G, Paganin P, Lopez L, Vanni C, Dalmastrì C, Cantale C, Daddiego L, Perrotta G, Dolce D, Morelli P, et al. Pyrosequencing unveils cystic fibrosis lung microbiome differences associated with a severe lung function decline. *PLoS One.* 2016;11(6):e0156807.
73. Woodruff PG, Modrek B, Choy DF, Jia G, Abbas AR, Ellwanger A, Koth LL, Arron JR, Fahy JV. T-helper type 2-driven inflammation defines major subphenotypes of asthma. *Am J Respir Crit Care Med.* 2009;180(5):388–95.

Submit your next manuscript to BioMed Central and we will help you at every step:

- We accept pre-submission inquiries
- Our selector tool helps you to find the most relevant journal
- We provide round the clock customer support
- Convenient online submission
- Thorough peer review
- Inclusion in PubMed and all major indexing services
- Maximum visibility for your research

Submit your manuscript at  
[www.biomedcentral.com/submit](http://www.biomedcentral.com/submit)

